

# CHEMISTRY

## A European Journal

A Journal of



### Accepted Article

**Title:** Nanoscale fluorescent MOF@microporous organic polymers composites for enhanced intracellular uptake and bioimaging

**Authors:** Lei Wang and Zhigang Xie

This manuscript has been accepted after peer review and appears as an Accepted Article online prior to editing, proofing, and formal publication of the final Version of Record (VoR). This work is currently citable by using the Digital Object Identifier (DOI) given below. The VoR will be published online in Early View as soon as possible and may be different to this Accepted Article as a result of editing. Readers should obtain the VoR from the journal website shown below when it is published to ensure accuracy of information. The authors are responsible for the content of this Accepted Article.

**To be cited as:** *Chem. Eur. J.* 10.1002/chem.201604416

**Link to VoR:** <http://dx.doi.org/10.1002/chem.201604416>

Supported by  
**ACES**

WILEY-VCH

# Nanoscale fluorescent MOF@microporous organic polymers composites for enhanced intracellular uptake and bioimaging

Lei Wang,<sup>[a]</sup> Weiqi Wang,<sup>[a],[b]</sup> Xiaohua Zheng,<sup>[a],[b]</sup> Zhensheng Li,<sup>[a]</sup> and Zhigang Xie\*<sup>[a]</sup>

**Abstract:** Polymer-modified metal-organic frameworks combine advantages of both soft polymers and crystalline metal-organic frameworks (MOFs). It is a big challenge to develop simple method for surface modification of MOFs. In this work, a MOFs@microporous organic polymers (MOPs) hybrids nanoparticle (UNP) has been synthesized by epitaxial growth of luminescent BODIPYs-imine MOPs on the surface of UiO-MOFs seeds, which exhibits low cytotoxicity, smaller size distribution, well-retained pore integrity and available functional sites. After folic acid grafting, the enhanced intracellular uptake and bioimaging was validated.

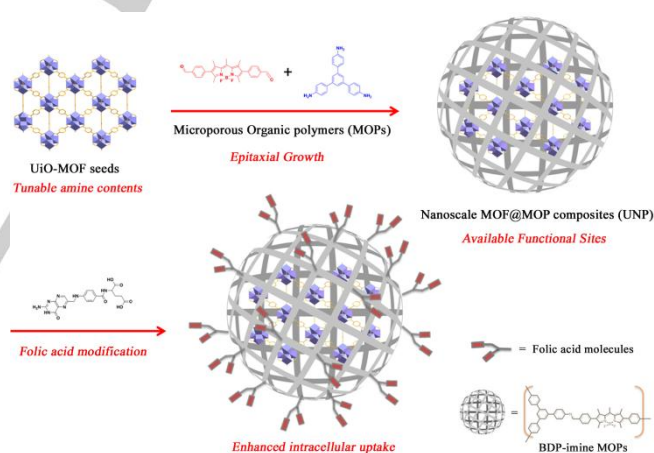
## Introduction

Metal-organic frameworks (MOFs) or Porous coordination polymers (PCPs), which constructed by the coordination bond driven self-assembly, are definitely as one of the most fascinating materials due to their tunable porous structures and intriguing properties.<sup>[1]</sup> The main limitation for the further potential applications of nanoscale metal-organic frameworks (NMOFs) lies with how to introduce new functionality and thus maintaining the intrinsic features. Much efforts have been devoted to alter the inner pore environment of MOFs through the pre-designed functional ligands<sup>[2]</sup> or post-synthetic methods.<sup>[3]</sup> However, the surface modification of MOFs remains less explored, and some of successful examples are heterogeneous core-shell MOFs single crystals<sup>[4]</sup> and polymers or lipids coating MOFs composites.<sup>[5]</sup> For biomedicine applications,<sup>[6]</sup> the surface modification of MOFs nanoparticles may dramatically enhance the bio-stability, drug loading and grafting targeting units.

On the other hands, microporous organic polymers (MOPs) represent another subclass of porous materials, which are covalently connected with organic building blocks to form two or three dimensional networks *via* coupling reactions.<sup>[7]</sup> The combined advantages from MOFs and MOPs in heterogeneous composite may provide some new synergy properties and thus extend the potential application.<sup>[8]</sup> Comparing with those classical coating materials, MOPs as surface modifying agents will not only regulate the chemical

environment on the surface of MOFs, but also keeps the pore integrity. Little has been done to prepare MOFs@MOPs core-shell nanoparticles in the literature. A very recent study of Son *et al.* succeeds in this aspect by coating NH<sub>2</sub>-UiO-66 nanoparticles with 8-30 nm thickness of MOPs layers by Sonogashira coupling of tetra(4-ethynylphenyl) methane and linear diiodo-substituted aromatic units.<sup>[9]</sup> After MOPs coating the hydrophobic character of MOFs dramatically change, and can be further used as adsorbents of toluene on water. In this regard, it is highly interesting to introduce new types of MOPs for coating MOFs nanoparticles and extending their potential applications, such as biomedicine.

In this paper, as shown in Scheme 1, the MOF@MOP hybrids nanoparticles (UNP) have been obtained by epitaxial growth of BODIPYs-imine based MOPs on the surface of pre-synthesized UiO-MOF seeds. Then, the biomolecule folic acid (FA) as an example has been successfully grafted *via* condensation of the rest aldehyde of UNP and amines groups of FA. Finally, the enhanced intracellular uptake and bioimaging of such modified UNP have been well demonstrated.



**Scheme 1.** Schematic presentation of MOF@MOP hybrids nanoparticles (UNP) synthesis and its application in enhanced intracellular uptake and bioimaging.

## Results and Discussion

Template synthesis is a straight forward approach for the shape and size control of resultant products.<sup>[10]</sup> The key for this approach is the size and the surface features (electronic charge, functional sites and hydrophilic/hydrophobic properties) of selected templates. For epitaxial growth, some chemical modification on the surface of templates, such as polyvinylpyrrolidone (PVP) or silica, are needed in order to enhance the interaction between templates and composition of

[a] Dr. L. Wang, Dr. W. Wang, Dr. X. Zheng, Dr. Z. Li, Prof. Z. Xie  
State Key Laboratory of Polymer Physics and Chemistry,  
Changchun Institute of Applied Chemistry, Chinese Academy of  
Sciences, Changchun 130022, P. R. China. Department  
E-mail: xiez@ciac.ac.cn

[b] Dr. W. Wang, X. Zheng  
Department The University of Chinese Academy of Sciences,  
Beijing 100049, P. R. China.

Supporting information for this article is given via a link at the end of the document.

coating layers.<sup>[11]</sup> Our present strategy for preparing MOFs@MOPs hybrids nanoparticles involves the selected synthesis of NMOFs seeds as self-templates with different contents of amine groups and then the growth of MOPs by condensation of amine and aldehyde groups. Highly crystallized UiO-66 and NH<sub>2</sub>-UiO-66 are initially prepared by modified solvothermal method. The content of amino groups is 0 and 100 mole % for UiO-66 and NH<sub>2</sub>-UiO-66, respectively. Furthermore, amine modified UiO-66 (UiO-AM) with 50 mole % of amino groups was made through solvent-assisted ligand exchange (Figure 1a). Detailed experimental processes are presented in the ESI section. Transmission electron microscopy (TEM) images of UiO-66, NH<sub>2</sub>-UiO-66 and UiO-AM nano-templates (Figure 1b) show well-defined cubical blocks shape with a mean diameter of ca. 70 nm. The octahedral shape and size of UiO-AM retain well after solvent-assisted ligands exchange approach. These UiO-MOFs are further used for growth of MOP. The crystallizability and structural stability of the as-synthesized UiO-MOFs templates are validated by powder X-ray diffraction (PXRD) (Figure S1). The successful ligands exchange of UiO-AM is determined by the liquid <sup>1</sup>H nuclear magnetic resonance (<sup>1</sup>H NMR), and the exchanged content of 2-aminoterephthalic acid (NH<sub>2</sub>-BDC) is about 50 % (Figure S2).

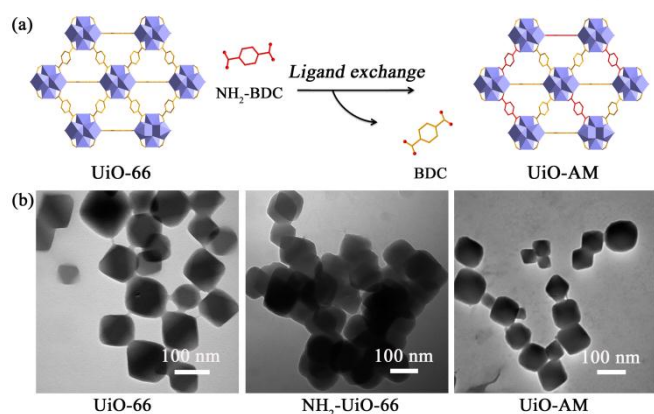


**Figure 1.** (a) Schematic presentation of UiO-AM synthesis by solvent-assisted ligand exchange. (b) TEM imagings of as-synthesized UiO-MOF templates, UiO-66, NH<sub>2</sub>-UiO-66 and UiO-AM. scale bar: 100 nm.

In order to confirm the successful formation of imine-containing MOF, the condensation of aniline with dialdehyde-substituted BODIPYs (CHO-BDP) was carried out as model reaction and further be characterized by <sup>1</sup>H NMR and Fourier transform infrared spectrometer (FTIR) (Figure S3-4). The condensation of cross-linker 1,3,5-tris(4-aminophenyl)benzene (TAPB) with CHO-BDP results in the construction of the {A<sub>3</sub>B<sub>2</sub>}-typed BDP-imine MOPs network with elimination of water. The successful formation of imine

bonds are confirmed by FTIR at 1607 and 1190 cm<sup>-1</sup> and solid <sup>13</sup>C nuclear magnetic resonance (solid <sup>13</sup>C NMR) at 160 ppm (Figure 2).<sup>[12]</sup> In typical synthesis of UNP hybrids nanoparticles, UiO-MOF nano-seeds were firstly well dispersed in a mixture solution of MeOH and CHCl<sub>3</sub>. Then stoichiometric ratio of CHO-BDP and TAPB were added and stirred at 70 °C for 48 hours. The color of UNP samples change from white to dark pink after BDP-imine MOP coating (Figure S5).

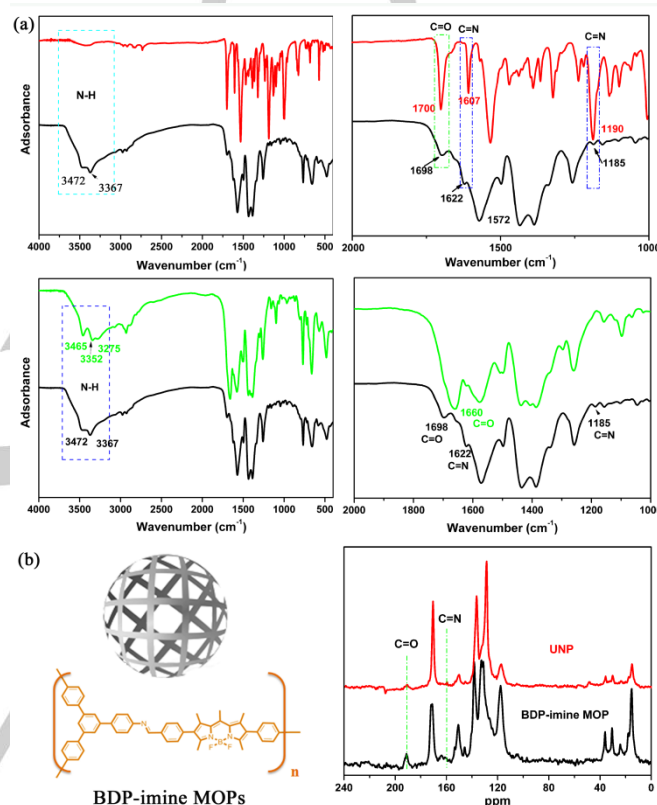


**Figure 2.** (a) FTIR spectra of UNP (black), BDP-imine MOPs (red) and UiO-AM (green) in KBr mode. (b) Schematic presentation of as-synthesized BDP-imine MOPs and the solid <sup>13</sup>C NMR spectra of UNP and BDP-imine MOP.

Pure BDP-imine MOPs with irregular blocks morphology are prepared in the absence of UiO-MOF, and their particles size are disordered distribution at micrometer level (Figure 3c and 3f). Another vital factor for synthesizing UNP nanoparticles is the content of amine groups in UiO-MOFs. With no amine groups on the surface of UiO-66 templates, none core-shell hybrids but the mixture of UiO-66 and BDP-imine MOPs are obtained by using UiO-66 seeds. While NH<sub>2</sub>-UiO-66 seeds with highest amine groups contents lead to form larger aggregates of final pink core-shell products as shown in Figure 3a and 3d, probably due to the poor dispersibility. For the UiO-AM seeds with 50 % amine groups contents, the size

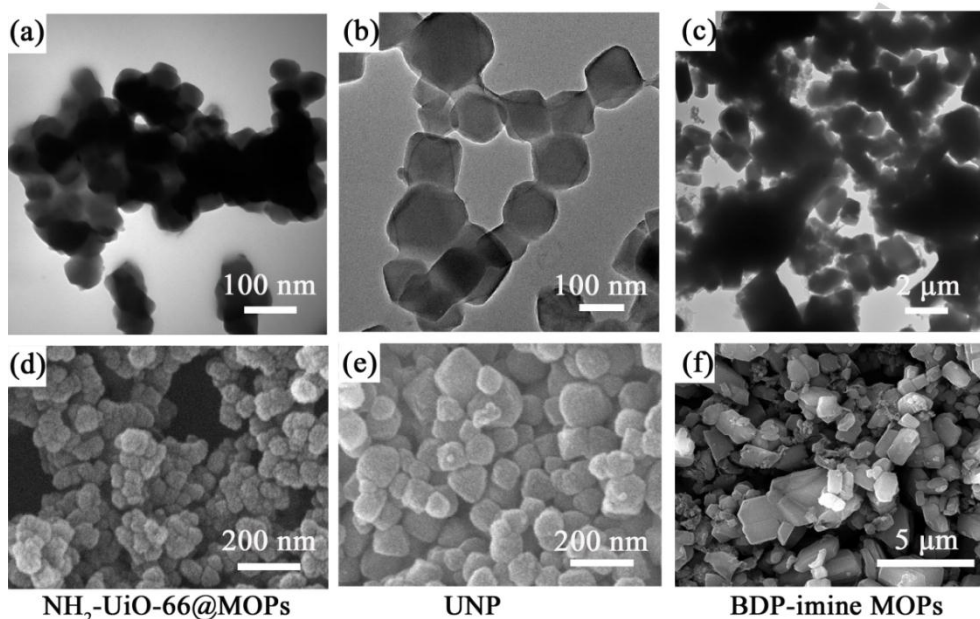


**Figure 3.** TEM and SEM imaging of as-synthesized MOFs@MOPs core-shell nanoparticles with or without UiO-MOFs templates, MOFs@MOPs obtained by  $\text{NH}_2\text{-UiO-66}$  as templates (a, d), UNP nanoparticles synthesized by UiO-AM seeds (b, e) and template-free BDP-imine MOPs (c, f).

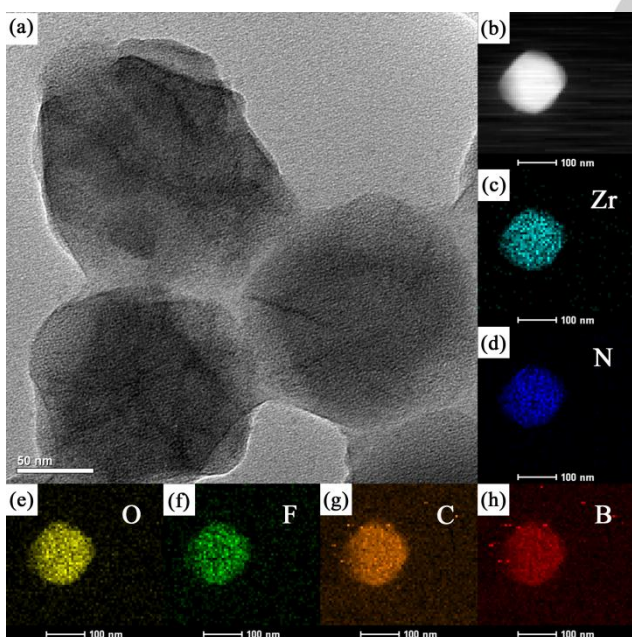


**Figure 4.** High-magnification TEM images (a-b) and EDS mapping images (c-h) of UNP nanoparticles by using UiO-AM as template. (Scale bar 50 nm; scale bar in the inset 100 nm).

of UNP nanoparticles increase slightly, and their shape turn from the well-defined cubic of UiO-AM to spherical shape (Figure 3b and 3e). The chemical composition of as-synthesized UNP nanoparticles was confirmed by energy

dispersive X-ray spectroscopy (EDS) (Figure 4). Those above results further demonstrate that the well-defined shape and size of selected UiO-MOFs seeds and the tunable organic functions on the outer-surface of nano-seeds are straight forward factors for the shape and size control of resultant core-shell composites.

The successful formation of UNP nanoparticles have been fully characterized by PXRD,  $\text{N}_2$  sorption and others spectra measurements. As shown in Figure 5a, the identical Bragg diffraction peaks of UiO-AM seeds and UNP products indicate that the epitaxial growth BDP-imine MOPs on the outer surface of UiO-AM seeds do not affect the crystalline structure of UiO-MOFs. The formed BDP-imine MOPs are in amorphous state, and no typical diffraction peaks are found. The permanent porosity and structural integrity of as-synthesized UNP nanoparticles have been examined by gas sorption measurements after degassed at 393 K for 12 hours. The  $\text{N}_2$  isotherm curve of UNP nanoparticles (Figure 5b) shows a rapid increasing in initial state and then continual increasing in the next pressure region, indicating the coexistence of microporous and mesoporous within as-synthesized materials. The calculated BET surface areas of UNP is  $657 \text{ m}^2\text{g}^{-1}$ , which is lower than UiO-AM seeds ( $1020 \text{ m}^2\text{g}^{-1}$ ) but higher than pure BDP-imine MOPs ( $129 \text{ m}^2\text{g}^{-1}$ ), respectively. The pore-size distribution of UNP after BDP-imine MOPs coating changes slightly (Figure S6). The as-synthesized UNP sample shows a similar weight-loss behavior as UiO-AM in thermogravimetric (TGA) curve, and the final coating content is about 8.2 wt% (Figure S7). After

MOPs coating, zeta potentials of UiO-AM and UNP (Figure S8) in water slightly increase from -17 mV to -19.2 mV.

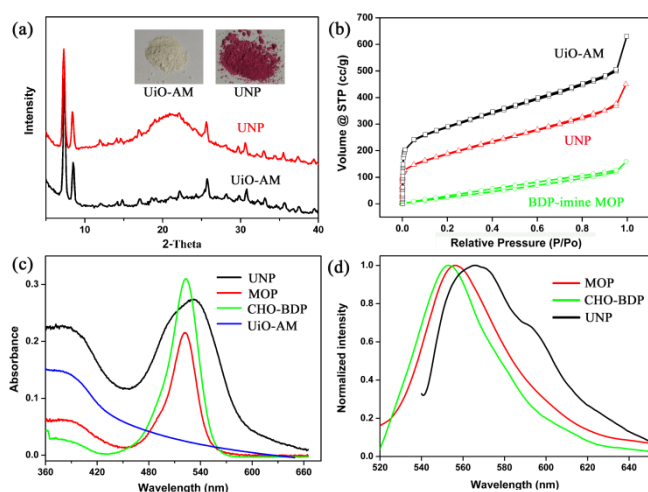


**Figure 5.** The characterization of as-synthesized MOF@MOP hybrids nanoparticles (UNP). (a) The powder X-ray diffraction of UiO-AM (black) and UNP (red). Inserted photograph of UiO-AM and UNP before and after BDP-imine MOPs coating. (b) Nitrogen adsorption isotherm curves of UiO-AM (black), UNP (red) and BDP-imine MOP (green) at 77 K. (c) UV absorption spectra of UNP (black), BDP-imine MOP (red), free CHO-BDP (green) and UiO-AM templates (blue) in DMF. (d) The luminescence spectra of UNP (black), BDP-imine MOP (red) and free CHO-BDP (green) dispersed into DMF,  $\lambda_{\text{exc}}$ : 520 nm.

The FTIR spectra of UNP nanoparticles (Figure 2a) show C=N stretching modes at 1622 and 1185  $\text{cm}^{-1}$  (1622 and 1192  $\text{cm}^{-1}$  in model compound, 1607 and 1190  $\text{cm}^{-1}$  in pure BDP-imine MOPs), clearly confirming the formation of imine bonds. Moreover, an aldehyde (C=O) stretch at 1698  $\text{cm}^{-1}$  for UNP and 1700  $\text{cm}^{-1}$  for BDP-imine MOPs can also be observed, indicating the presence of unreacted aldehyde groups from CHO-BDP reactant. No unreacted amine groups are existed, as evidenced by the two broad spikes from 3200 to 3700  $\text{cm}^{-1}$ . The solid  $^{13}\text{C}$  NMR spectrum of UNP (Figure 2b) further validates the growth of BDP-imine MOPs on the UiO-MOF surface with C=N resonance at 160 ppm. A carbonyl peak with C=O resonance at 195 ppm is also observed and attributed to unreacted aldehyde groups. In contrast to the CHO-BDP, the UV spectrum of UNP dispersed in DMF gives a minor shift from 522 nm to 531 nm (Figure 5c), while its corresponding luminescence spectrum excited at 520 nm exhibiting an obvious red-shift from 552 nm to 566 nm (Figure 5d). We suppose that the red-shift behavior may be ascribed to the interaction on the formed interface between the MOF templates and MOP shell. Meanwhile, the fluorescence quantum yields ( $\Phi$ ) of free CHO-BDP, BDP-imine MOPs and UNP nanoparticles in MeOH (Rhodamine 6G as reference)<sup>[13]</sup> are determined and given the value of 1.024, 0.027 and 0.163, respectively. In contrast with most

reported polymers modified MOFs,<sup>[5]</sup> the as-synthesized UNP composite after the BDP-imine MOPs growth not only retains the well size distribution, permanent porosity and structural integrity as previous UiO-MOFs templates, but also successfully introduces luminescence as new function into MOFs and expands potential applications.

Bioconjugate of drugs, macromolecules and nanoparticles with FA have been reported to target cell membrane and to enhance their uptake *via* the folate receptor, which is overexpressed by some cancer cells.<sup>[14]</sup> FA-modified UNP samples with different FA contents, named UNP-10FA and UNP-20FA, have been prepared by condensation reaction of retained aldehyde groups on the outer-surface of as-synthesized UNP with the amine groups of FA molecules. The successful modification was determined by FTIR (Figure S9) and UV spectrum (Figure S10). FA content was determined according to the standard curves of UV-Vis in DMF. After FA grafting, zeta potentials of FA-modified UNP samples (Figure S8) in water change negligibly.

To evaluate the biocompatibility of as-synthesized UNP and FA-modified UNP samples, the standard 3-(4,5-dimethylthiazol-2-yl)-2,5-diphenyltetrazolium bromide (MTT) proliferation test versus different incubation concentrations against living human lung cancer cell (A549), human cervix Carcinoma cells (HeLa) and human nasopharyngeal carcinoma cells (KB) have been carried out. No significant cell cytotoxicity of UNP and FA-modified UNP nanoparticles have been observed, and more than 95 % of examined cells are alive below the concentration of 10  $\mu\text{g mL}^{-1}$  after incubation of 24 hours at 37  $^{\circ}\text{C}$  (Figure S11). Hence, the as-synthesized UNP, UNP-10FA and UNP-20FA nanoparticles with low cytotoxicity can be further applied in biological systems.

The confocal laser scanning microscopy (CLSM) was used to study the cellular uptake of as-synthesized samples with different FA contents. As shown in Figure 6, A549, HeLa and KB cells were visualized by DAPI ( $\lambda_{\text{exc}}$  405 nm) in the blue channel and UNP ( $\lambda_{\text{exc}}$  488 nm) in the red channel, respectively. UNP and FA-modified UNP nanoparticles with the same CHO-BDP concentration of 1  $\mu\text{g mL}^{-1}$  have been incubated with above selected cells line for 24 hours. The red luminescence mainly located in cell cytoplasm, indicating that all samples can pass across the cell membrane into cytoplasm. Moreover, cellular uptakes of all samples largely enhanced with the increasing FA contents. With the aim to further compare and quantify the cellular uptake, flow cytometry experiments (Figure 6 and Figure S12) have been carried out based on the average luminescent intensity of CHO-BDP composition. After FA grafted, the cellular uptake of as-synthesized nanoparticles on HeLa and KB cell lines are higher than A549 cell lines. At the highest FA contents of 20 %, the calculated uptake rates are 2.1-fold for HeLa, 2.2-fold for KB and 1.7-fold for A549, respectively.

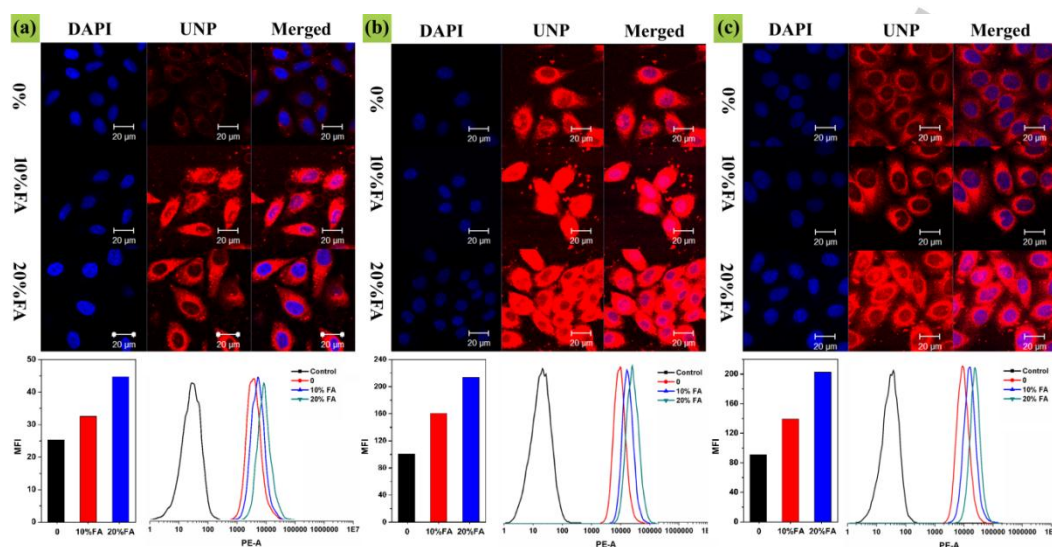


**Figure 6.** *In vitro* CLSM images, flow cytometry analyses and mean fluorescence intensity (MFI) quantification of A549 cells (a), HeLa cells (b) and KB cells (c) treated with UNP, UNP-10FA and UNP-20FA with the same CHO-BDP concentration of  $1 \mu\text{g mL}^{-1}$  for 2 h at  $37^\circ\text{C}$ . Scale bars:  $20 \mu\text{m}$ .

## Conclusions

In conclusion, we have developed a versatile and simple template controlled approach for design and preparation of the heterogeneous MOF@MOP hybrid nanoparticles with low cytotoxicity, smaller size, luminescence and well-retained pore integrity. The as-synthesized core-shell nanoparticle can be further applied as nanoplatform for bio-imaging and enhanced cellular uptake *via* modification of folic acid. A sound proof for the synergy between two types of porous materials open a new way for chemical modification of MOF materials and also for preparation of nanosized porous polymers.

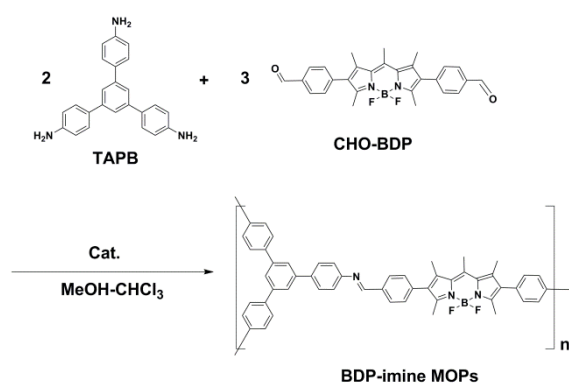
## Experimental Section

**Materials and Methods.** All starting materials were commercially available and used without further purification. CHO-BDP and 1,3,5-tris(4-aminophenyl)benzene (TAPB) were synthesized according to previous work.<sup>[15]</sup> N,N-dimethylformamide (DMF) was stored over activated molecular sieves and was distilled under reduced pressure. Ultrapure water was prepared using a Millipore Simplicity System (Millipore, Bedford, USA). FTIR was measured by Nicolet Impact 410 Fourier transform infrared spectrometer. UV and Fluorescence were recorded on SHIMADZU UV-2450 and Edinburgh Instrument FLS-920 spectrometer, respectively. TEM and SEM images were recorded by JEOL JEM-1011 electron microscope (acceleration voltage of 100 kV) and JEOL JXA-840 (acceleration voltage of 15 kV). The size distribution and zeta potential were measured by Malvern Zeta Seizer-Nano ZS90 instrument. The Solid-state  $^{13}\text{C}$  and  $^1\text{H}$  NMR spectra were recorded at 5K Hz. PXRD was performed by a Bruker D8 diffractometer using Cu-K $\alpha$  radiation, 40 kV, 40 mA with scanning rate of  $1.0^\circ/\text{min}$ . The thermogravimetric analysis (TGA) was performed using a Netzsch Sta 449c thermal analyzer system at a rate of  $10^\circ\text{C}/\text{min}$  under air

atmosphere. The nitrogen adsorption isotherm was measured on a Micrometrics ASAP 2010 analyzer.

**Synthesis of UiO-MOF templates.** UiO-66 and  $\text{NH}_2$ -UiO-66 were synthesized by previous work.<sup>[3c, 16]</sup> UiO-AM was synthesized by the solvent-assisted ligands exchange approach.  $\text{NH}_2$ -BDC (36 mg) and UiO-66 (28 mg) were well dispersed into 2 mL DMF and then stirred at  $85^\circ\text{C}$  for 48 hours. After cooling, the white powders were collected by centrifugation ( $12000 \text{ rpm} \times 10 \text{ min}$ ), washed with DMF and methanol for several times and dried under vacuum.

**Synthesis of model compound.** 2 equal aniline and 1 equal CHO-BDP were added into the mixed solvent of MeOH and  $\text{CHCl}_3$ . After adding amount of 6 M HAc catalysis, this mixture was heating at  $70^\circ\text{C}$  overnight. After cooling, the powders were collected for further characterization.



**Scheme 2.** Schematic presentation of BDP-imine MOPs.

**Synthesis of BDP-imine MOPs.** 2 equal TAPB and 3 equal CHO-BDP were added into the mixed solvent of MeOH and  $\text{CHCl}_3$ . After adding

amount of 6 M HAc catalysis, this mixture was heating at 70 °C for 48 h. After cooling, the red-purple powders were collected for characterization.

**Synthesis of MOF@MOP hybrids nanoparticles.** In typical synthesis of MOF@MOP hybrids nanoparticles, UiO-MOF nano-seeds (20 mg for UiO-66, NH<sub>2</sub>-UiO-66 and UiO-AM) were firstly well dispersed in mixture solutions of MeOH and CHCl<sub>3</sub>. CHO-BDP (4 mg), TAPB (1 mg) and three drops of 6 M HAc were added and heated at 70 °C for 48 hours. After cooling, the dark pink powders were collected by centrifugation (12000 rpm × 10 min), washed with methanol for several times and dried under vacuum.

**Synthesis of FA-modified MOF@MOP hybrids nanoparticles.** In typical synthesis of FA-modified MOF@MOP hybrids nanoparticles, 10 mg of as-synthesized UNP samples were firstly well dispersed in mixture solutions of MeOH and DMF. Folic acids (1 mg for 10 wt% and 2 mg for 20 wt%) and three drops of 6 M HAc were added and heated at 70 °C for 48 hours. After cooling, the dark pink powders were collected by centrifugation (12000 rpm × 10 min), washed with MeOH and DMF for several times and dried under vacuum.

**Cell culture.** Human Cervix Carcinoma cells (HeLa), human lung cancer cell (A549) and human nasopharyngeal carcinoma cell (KB) were cultured in dulbecco minimum essential medium (DMEM) medium without folic acid supplemented with 10 % (v/v) fetal calf serum. Cell were grown in a humidified incubator at 37 °C in 5 % CO<sub>2</sub> atmosphere. The medium was replaced every two days and cells were subcultured by trypsinization.

**Confocal laser scanning microscopy (CLSM).** The above cells were seeded into 6-well plates at an initial cell density of 1 × 10<sup>5</sup> cells/well in 2 mL of DMEM medium. The cells were treated with or without folic acid modified UNP samples at the same CHO-BDP concentration of 1 µg mL<sup>-1</sup> at 37 °C. After 24 h incubation, the cell culture medium was removed and cells were washed with ice-cold PBS buffer (pH = 7.4) for twice times before fixed with fresh 4.0 % paraformaldehyde (1 mL) for 10 min at room temperature. The cells were counterstained with DAPI for cell nucleus. The fixed cells were again washed with PBS 7.4 for three times before observation by confocal laser scanning microscope (Carl Zeiss LSM 780).

**Cellular uptake by flow cytometry.** HeLa, A549 and HepG2 cells were seeded in six-well plates (2 × 10<sup>5</sup> cells / well) and grown in complete DMEM medium for 24 h. The with or without folic acid modified UNP samples at the same CHO-BDP concentration of 1 µg mL<sup>-1</sup> in fresh culture medium were added into each well. After incubation for 24 h at 37 °C, the medium was removed and cells washed three times with cold PBS before trypsin treatment. The collected cells were centrifuged at 1000 rpm for 5 min and washed by PBS twice. The supernatants were discarded and the cell pellets were re-suspended in 0.5 mL PBS 7.4. Flow cytometer analysis was performed by a flow cytometer (Beckman, USA) which collected 1 × 10<sup>4</sup> gated events for each sample.

**Cytotoxicity assay.** The dark cytotoxicity of free CHO-BDP and UNP samples with or without modified folic acid (FA) were evaluated by 3-(4,5-dimethylthiazol-2-yl)-2,5-diphenyltetrazolium bromide (MTT) assay.<sup>[17]</sup> Cells harvested in a logarithmic growth phase were seeded in 96-well plates at a density of 10<sup>4</sup> cells / well and incubated overnight. Then different concentrations of samples were added into each well and incubated for 48 h. After the removal of nanoparticles, cells were transferred into fresh media before 20 µL of MTT (5 mg/mL) was added. Then, the plates were incubated for another 4 h at 37 °C, followed by removal of the culture medium containing MTT and addition of 150 µL of

DMSO to each well. Finally, the plates were shaken for 5 min, and the absorbance at 490 nm was recorded by a microplate reader.

## Acknowledgements

Financial support was kindly provided by the National Natural Science Foundation of China (Project No. 21401188 and 51522307).

**Keywords:** Metal-Organic Frameworks (MOFs) • Microporous Organic Polymers (MOPs) • bioimaging • cellular uptake

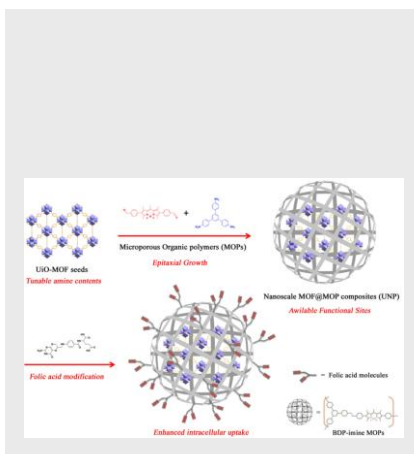
- [1] (a) J. R. Long and O. M. Yaghi, *Chem. Soc. Rev.*, **2009**, *38*, 1213-1214; (b) H.-C. Zhou, J. R. Long and O. M. Yaghi, *Chem. Rev.*, **2012**, *112*, 673-674; (c) L. Wang, W. Wang and Z. Xie, *J. Mater. Chem. B*, **2016**, *4*, 4263-4266.
- [2] M. C. Das, S. Xiang, Z. Zhang and B. Chen, *Angew. Chem. Int. Ed.*, **2011**, *50*, 10510-10520.
- [3] (a) S. M. Cohen, *Chem. Rev.*, **2012**, *112*, 970-1000; (b) O. Karagiari, W. Bury, J. E. Mondloch, J. T. Hupp and O. K. Farha, *Angew. Chem., Int. Ed.*, **2014**, *53*, 4530-4540. (c) W. Wang, L. Wang, Z. Li, Z. Xie, *Chem. Commun.*, **2016**, *52*, 5402-5405.
- [4] (a) S. Furukawa, K. Hirai, K. Nakagawa, Y. Takashima, R. Matsuda, T. Tsuruoka, M. Kondo, R. Haruki, D. Tanaka, H. Sakamoto, S. Shimomura, O. Sakata and S. Kitagawa, *Angew. Chem. Int. Ed.*, **2009**, *48*, 1766-1770; (b) K. Koh, A. G. Wong-Foy and A. J. Matzger, *Chem. Commun.*, **2009**, *45*, 6162-6124; (c) L. Wang, W. Yang, Y. Li, Z. Xie, W. Zhu and Z. M. Sun, *Chem. Commun.*, **2014**, *50*, 11653-11656.
- [5] (a) M. S. Denny and S. M. Cohen, *Angew. Chem. Int. Ed.*, **2015**, *54*, 9029-9032; (b) K. A. McDonald, J. I. Feldblyum, K. Koh, A. G. Wong-Foy and A. J. Matzger, *Chem. Commun.*, **2015**, *51*, 11994-11996; (c) S. Wang, W. Morris, Y. Liu, C. M. McGuirk, Y. Zhou, J. T. Hupp, O. K. Farha and C. A. Mirkin, *Angew. Chem. Int. Ed.*, **2015**, *54*, 14738-14742; (d) Z. Zhang, H. T. Nguyen, S. A. Miller, A. M. Ploskonka, J. B. DeCoste and S. M. Cohen, *J. Am. Chem. Soc.*, **2016**, *138*, 920-925; (e) W. Wang, L. Wang, Y. Li, S. Liu, Z. Xie and X. Jing, *Adv. Mater.*, **2016**, *28*, 9320-9325.
- [6] (a) W. J. Rieter, K. M. Pott, K. M. L. Taylor and W. Lin, *J. Am. Chem. Soc.*, **2008**, *130*, 11584-11585; (b) D. Liu, C. Poon, K. Lu, C. He and W. Lin, *Nat. Commun.*, **2014**, *5*, 4182-4192; (c) W. Wang, L. Wang, Y. Huang, Z. Xie and X. Jing, *Chem. Asian J.* **2016**, *11*, 750-756. (d) M. Zheng, S. Liu, X. Guan and Z. Xie, *ACS Appl. Mater. Interfaces* **2015**, *7*, 22181-22187.
- [7] (a) F. J. Uribe-Romo, J. R. Hunt, H. Furukawa, C. Klöck, M. O'Keeffe and O. M. Yaghi, *J. Am. Chem. Soc.*, **2009**, *131*, 4570-4571; (b) X. Feng, X. Ding and D. Jiang, *Chem. Soc. Rev.*, **2012**, *41*, 6010-6022; (c) S. Y. Ding and W. Wang, *Chem. Soc. Rev.*, **2013**, *42*, 548-568; (d) M. G. Rabbani, A. K. Sekizkardes, Z. Kahveci, T. E. Reich, R. Ding, and H. M. El-Kaderi, *Chem. Eur. J.*, **2013**, *19*, 3324-3328; (e) Q. Fang, S. Gu, J. Zheng, Z. Zhuang, S. Qiu and Y. Yan, *Angew. Chem. Int. Ed.*, **2014**, *53*, 2878-2882; (f) H. A. Patel, S. Je, J. Park, Y. Jung, A. Coskun, and C. T. Yavuz, *Chem. Eur. J.*, **2014**, *20*, 772-780; (g) X. Chen, M. Addicoat, E. Jin, L. Zhai, H. Xu, N. Huang, Z. Guo, L. Liu, S. Irle and D. Jiang, *J. Am. Chem. Soc.*, **2015**, *137*, 3241-3247; (h) D. B. Shinde, S. Kandambeth, P. Pachfule, R. R. Kumar and R. Banerjee, *Chem. Commun.*, **2015**, *51*, 310-313; (i) R. S. Sprick, J.-X. Jiang, B. Bonillo, S. Ren, T. Ratvijitvech, P. Guignon, M. A. Zwijnenburg, D. J. Adams and A. I. Cooper, *J. Am. Chem. Soc.*, **2015**, *137*, 3265-3270.
- [8] (a) K. Qian, G. Fang and S. Wang, *Chem. Commun.*, **2011**, *47*, 10118-10120; (b) M. s. L. Pinto, S. Dias and J. Pires, *ACS Appl. Mater.*

- Interfaces*, **2013**, *5*, 2360-2363; (c) J. Fu, S. Das, G. Xing, T. Ben, V. Valtchev and S. Qiu, *J. Am. Chem. Soc.*, **2016**, *138*, 7673-7680.
- [9] J. Chun, S. Kang, N. Park, E. J. Park, X. Jin, K. D. Kim, H. O. Seo, S. M. Lee, H. J. Kim, W. H. Kwon, Y. K. Park, J. M. Kim, Y. D. Kim and S. U. Son, *J. Am. Chem. Soc.*, **2014**, *136*, 6786-6789.
- [10] (a) C. Jo, H. J. Lee and M. Oh, *Adv. Mater.*, **2011**, *23*, 1716-1719; (b) Li and H. C. Zeng, *J. Am. Chem. Soc.*, **2014**, *136*, 5631-5639; (c) X. Zhuang, D. Gehrig, N. Forler, H. Liang, M. Wagner, M. R. Hansen, F. Laquai, F. Zhang and X. Feng, *Adv. Mater.*, **2015**, *27*, 3789-3796.
- [11] (a) G. Lu, S. Li, Z. Guo, O. K. Farha, B. G. Hauser, X. Qi, Y. Wang, X. Wang, S. Han, X. Liu, J. S. DuChene, H. Zhang, Q. Zhang, X. Chen, J. Ma, S. C. Loo, W. D. Wei, Y. Yang, J. T. Hupp and F. Huo, *Nat. Chem.*, **2012**, *4*, 310-316; (b) Y. Chen, X. Huang, X. Feng, J. Li, Y. Huang, J. Zhao, Y. Guo, X. Dong, R. Han, P. Qi, Y. Han, H. Li, C. Hu and B. Wang, *Chem. Commun.*, **2014**, *50*, 8374-8377.
- [12] (a) P. Pandey, A. P. Katsoulidis, I. Eryazici, Y. Wu, M. G. Kanatzidis and S. T. Nguyen, *Chem. Mater.*, **2010**, *22*, 4974-4979; (b) Y. Zhu, H. Long and W. Zhang, *Chem. Mater.*, **2013**, *25*, 1630-1635.
- [13] I. John Olmsted, *J. Phys. Chem.* **1979**, *83*, 2581-2584.
- [14] (a) M. Quaglia, K. Chenon, A. J. Hall, E. D. Lorenzi and B. Sellergren, *J. Am. Chem. Soc.*, **2001**, *123*, 2146-2154; (b) P. S. Low, W. A. Henne and D. D. Doorneweerd, *Acc. Chem. Res.*, **2008**, *40*, 120-129; (c) R. I. Pinhassi, Y. G. Assaraf, S. Farber, M. Stark, D. Ickowicz, S. Drori, A. J. Domb and Y. D. Livney, *Biomacromolecules*, **2010**, *11*, 294-303; (d) S.-J. Yang, F.-H. Lin, K.-C. Tsai, M.-F. Wei, H.-M. Tsai, J.-M. Wong and M.-J. Shieh, *Bioconjugate Chem.*, **2010**, *21*, 679-689; (e) E. Roger, S. Kalscheuer, A. Kirtane, B. R. Guru, A. E. Grill, J. Whittum-Hudson and J. Panyam, *Mol. Pharm.*, **2012**, *9*, 2103-2110; (f) M. A. van Dongen, J. E. Silpe, C. A. Dougherty, A. K. Kanduluru, S. K. Choi, B. G. Orr, P. S. Low and M. M. Banaszak Holl, *Mol. Pharm.*, **2014**, *11*, 1696-1706.
- [15] (a) T. Yogo, Y. Urano, Y. Ishitsuka, F. Maniwa, T. Nagano, *J. Am. Chem. Soc.*, **2005**, *127*, 12162-12163; (b) D. Alejandro, R. David, S. Kyriakos C., C. Massimiliano, G. Denis, L. Fabiola, M. Silvia, R. Otello Maria, R. Maria Luisa, C. Carlos, M. Daniel, M. Rubn, S. Jos Luis, Z. Flix, *Chem. Eur. J.*, **2015**, *21*, 10666-10670.
- [16] J. H. Cavka, S. Jakobsen, U. Olsbye, N. Guillou, C. Lamberti, S. Bordiga and K. P. Lillerud, *J. Am. Chem. Soc.*, **2008**, *130*, 13850-13851.
- [17] T. Mosmann, *J. Immunol. Methods*. **1983**, *65*, 55-63.

## Entry for the Table of Contents

## FULL PAPER

A MOF@MOPs composite with low cytotoxicity, smaller size distribution, well-retained pore integrity and available functional sites has been synthesized by epitaxial growth of luminescent BODIPYs-imine MOPs on the surface of UiO-MOFs seeds. After folic acid grafting, the enhanced intracellular uptake and bioimaging was validated.



L. Wang, W. Wang, X. Zheng, Z. Li and Z. Xie\*

Page No. – Page No.

**Nanoscale fluorescent MOF@microporous organic polymers composites for enhanced intracellular uptake and bioimaging**